

Sensitivity analysis and Taguchi application in vacuum membrane distillation

Sushant Upadhyaya¹, Kailash Singh^{*1}, Satyendra Prasad Chaurasia¹, Rakesh Baghel¹,
Jitendra Kumar Singh² and Rajeev Kumar Dohare¹

¹Department of Chemical Engineering, Malaviya National Institute of Technology, Jaipur-302017, India

²Department of Chemical Engineering, JK Lakshmi Pat University, Jaipur-302026, India

(Received February 11, 2017, Revised July 20, 2018, Accepted July 23, 2018)

Abstract. In this work, desalination experiments were performed on vacuum membrane distillation (VMD). Process parameters such as feed flow rate, vacuum degree on permeate side, feed bulk temperature and feed salt concentration were optimized using sensitivity analysis and Taguchi method. The optimum values of process parameters were found to be 2 lpm of feed flow rate, 60°C of feed bulk temperature, 5.5 kPa of permeate-side pressure and 5000 ppm of salt concentration. The permeate flux at these conditions was obtained as 26.6 kg/m²-hr. The rejection of salt in permeate was found to be 99.7%. The percent contribution of various process parameters using ANOVA results indicated that the most important parameter is feed bulk temperature with its contribution of 95%. The ANOVA results indicate that the percent contribution of permeate pressure gets increased to 5.384% in the range of 2 to 7 kPa as compared to 0.045% in the range of 5.5 to 7 kPa.

Keywords: vacuum membrane distillation (VMD); sensitivity analysis; desalination; Taguchi method; ANOVA

1. Introduction

Membrane distillation (MD) is a thermally driven process, in which only vapor molecules are transported through porous hydrophobic membranes. The liquid feed to be treated by MD must be in direct contact with one side of the membrane and does not penetrate inside the dry pores of the membranes. The basic driving force for MD is the trans-membrane vapor pressure difference, which may be created towards downstream side of the membrane module (El-Bourawi *et al.* 2006). The water availability for human use is declining rapidly due to gradual rising of environmental pollution. According to world health organization (WHO), 1.1 billion people have no access to any type of improved drinking source of water (http://www.who.int/water_sanitation_health/mdg1/en/). Desalination can be classified in two broad areas as firstly phase change/thermal separation process like multi-effect boiling, vapor compression, freezing and solar stills and secondly membrane based separation process like membrane distillation, microfiltration (MF), ultra-filtration (UF), nanofiltration (NF) and reverse osmosis (RO). Membrane distillation, ion-exchange, reverse osmosis (RO), & electro dialysis are the various techniques for treatment of water by lowering the concentration of different multi-ions within the permissible limit for drinking. The energy required to run the desalination plants remains a drawback under thermal process except membrane distillation (MD), which does not require the feed to bring to its boiling point. RO process also requires use of high pressure pump and

hence viability for the rural areas is doubtful in absence of regular electricity supply. Also there is 60% rejection of water in RO membrane desalination, which poses problem for management of reject water (Chaurasia *et al.* 2013). Contrary to this, the use of MD for desalination has negligible water rejection problem and it can also be run without electricity using potential / solar energy which is easily available in rural areas.

MD is an emerging technology for desalination. It differs from the other membrane technologies in that the driving force for desalination is the difference in vapor pressure of water across the membrane, rather than total pressure. The membranes for MD are hydrophobic of micro-porous range, which permits water vapor to get through membrane rather than liquid water. The feed water is heated to establish the vapor pressure gradient, as a result it will elevate its vapor pressure. Many methods have been used to create the vapor pressure difference across the micro-porous hydrophobic membranes and in all cases, the saline feed water is fed to the hot side of the membrane directly for desalination purpose through MD (Walton *et al.* 2004). The simultaneous heat and mass transfer are involved through micro-porous hydrophobic membrane in MD process. The heat is transported through membrane pores as well as membrane material but mass transport takes place through the membrane pores only in MD process. The heat transfer inside the membrane pore is due to the vapor flux and latent heat of volatile component. Heat transfer through membrane material is by conduction (Khayet 2011). Various heat and mass transfer correlations were developed to estimate the effect of heat transfer and mass transfer coefficient on different operating parameters such as feed bulk temperature by various researchers (Izquierdo-Gil *et al.* 2008, Soni *et al.* 2008, Upadhyaya *et al.* 2016b).

*Corresponding author, Ph.D.
E-mail: ksingh.chem@mnit.ac.in

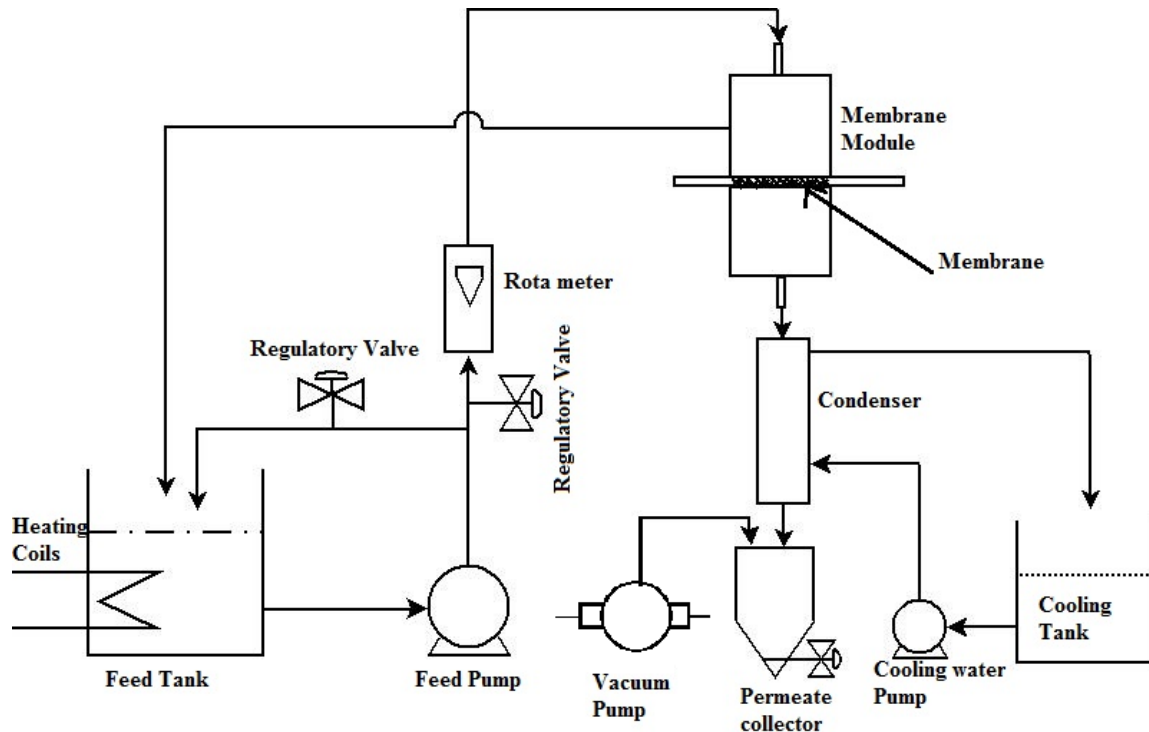


Fig. 1 Schematic diagram of vacuum membrane distillation set up

Four configurations were described by Alkhudhiri *et al.* (2012) to conduct MD process. These are direct contact membrane distillation (DCMD), sweeping gas membrane distillation (SGMD), air gap membrane distillation (AGMD), and vacuum membrane distillation (VMD). The difference among these configurations is the method in which the vapor molecule is condensed. In VMD, the boundary layer resistance in the permeate side and the contribution of the heat transported by conduction through the membrane are frequently neglected (Abu-Zeid *et al.* 2015, Bandini *et al.* 1997, Criscuoli *et al.* 2013, El-Bourawi *et al.* 2006, Lawson and Lloyd 1997, Shim *et al.* 2014). This makes VMD of pure water useful to determine the temperature of the feed solution at the membrane surface (T_{fm}) as it cannot be measured directly and therefore the boundary layer heat transfer coefficients in the membrane module can be evaluated (Mengual *et al.* 2004).

Many researchers (Banat *et al.* 2003, Bandini *et al.* 1997, Bandini and Sarti 1999, Bouguecha *et al.* 2003, Izquierdo-Gil and Jonsson 2003, Lawson and Lloyd 1997, Lovineh *et al.* 2013, Naidu *et al.* 2014, Pangarkar *et al.* 2010) have used the mathematical models based on the gas permeation through a porous membrane comprising Knudsen flow, while others (Mengual *et al.* 2004, Xu *et al.* 2009) frequently employed the model based on the combination of Knudsen-Poiseuille flow to calculate the VMD flux. However, Upadhyaya *et al.* (2016a) has reported model considering that the gas permeates through a porous membrane comprising Knudsen, molecular and Poiseuille flow.

Since, the permeate flux in VMD is affected by many parameters such as permeate side pressure, feed temperature, pore diameter, membrane characteristics parameters, etc., therefore, performance of each parameter

is needed to investigate theoretically using sensitivity analysis (Varma *et al.* 2005) and to find the optimum condition for process which relate the parameter and system performance. Many researchers (Kuram *et al.* 2013, Mehat and Kamaruddin 2011, Mohammadi and Safavi 2009) used Taguchi method as an important tool to produce high quality products with minimum runs. Taguchi methods enable researchers, designers and engineers to identify 'noise variable', which if not controlled can affect performance and quality.

In this paper, experimental data have been obtained for permeate flux by changing the process parameters *viz.* feed flow rate, feed bulk temperature, permeate pressure and feed salt concentration. Sensitivity analysis has been carried out to obtain the values of parameters at which the system is stabilized and less sensitive. Taguchi method has been applied by considering L_9 orthogonal array (4 factors and 03 levels) on experimental data to estimate the optimum process parameters. The authors could not find any work illustrating sensitivity analysis and Taguchi method simultaneously to investigate the optimum performance of VMD. ANOVA analysis has also been carried out to determine the percent contribution of each parameter on permeate flux.

2. Experimental

A Lab scale vacuum membrane distillation setup was used in the study. The schematic diagram of the experimental setup is shown in Figure 1. An aqueous NaCl feed solution was prepared and continuously fed through a feed tank to the membrane module by feed pump (0.37/0.50 HP of Crompton make). The excess flow was bypassed to

Table 1 Membrane characteristics

Property	Specifications
Material	Hydrophobic PTFE
Pore size, μm	0.22
Porosity, %	70
Thickness, μm	175

keep the feed flow rate constant. The membrane purchased from Millipore was made of hydrophobic PTFE microporous flat sheet membrane of effective diameter of 52 mm and its properties are reported in Table 1. On the permeate side of the membrane module, the vacuum pump (FRACOVAC make) was connected. The permeate water vapor was condensed continuously in a condenser using cooling water from tap. The membrane flux was measured by collecting permeate in a graduated receiver under steady state condition. The temperature controller equipped with heater was connected to maintain the temperature of the feed solution in the feed tank. Electrical conductivity of the membrane distillate permeate was measured using a multi-ion meter.

3. Sensitivity analysis

3.1 Theoretical discussion

The behavior of VMD is affected by many parameters such as permeate side pressure, feed temperature, pore diameter, membrane characteristics parameters, etc. When a system operates in the parametrically sensitive region, its performance changes sharply with small variation in parameters. Sensitivity analysis quantifies the relationship between the system behavior and a parameter. The normalized sensitivity of a variable y with respect to parameter p is defined as

$$S(y, p) = \frac{\partial \ln y}{\partial \ln p}$$

The mass flux model developed by Upadhyaya *et al.* (2016a) is

$$N_{A,M-K-P} = \frac{\varepsilon}{\tau \delta RT_{fm}} \left\{ \frac{1 - y_A}{D_{AB}} + \frac{3}{4d} \sqrt{\frac{2\pi M}{RT_{fm}}} \right\}^{-1} (P_{fm} - P_{pm}) + \frac{\varepsilon r^2}{\tau \delta} \frac{P_{fm} M}{8\eta RT_{fm}} (P_{fm} - P_{pm}) \quad (1)$$

To study the sensitivity of various parameters to the mass flux (N), the following sensitivity factors were derived from the mathematical model.

The normalized Sensitivity of mass flux to the membrane characteristics is given by

$$S\left(N, \frac{\varepsilon}{\tau \delta}\right) = \frac{\partial \ln N}{\partial \ln \frac{\varepsilon}{\tau \delta}} = 1 \quad (2)$$

Sensitivity of mass flux to the membrane pore diameter (d) is given by,

$$S(N, d) = \frac{\partial \ln N}{\partial \ln d} = \frac{4dc + 2fd^2 (bd + c)^2}{[4d + fd^2 (bd + c)](bd + c)} \quad (3)$$

where

$$b = \frac{1 - y_A}{D_{AB}}, c = \frac{3}{4} \sqrt{\frac{2\pi M}{RT_{fm}}}, f = \frac{P_{fm} M}{8\eta}$$

Sensitivity of mass flux to the permeate side membrane pressure is given by,

$$S(N, P_{pm}) = \frac{\partial \ln N}{\partial \ln P_{pm}} = -\frac{P_{pm}}{P_{fm} - P_{pm}} \quad (4)$$

Sensitivity of mass flux to the feed side membrane temperature is,

$$S(N, T_{fm}) = \frac{T_{fm}}{N} \frac{\partial N}{\partial T_{fm}} \quad (5)$$

where

$$\frac{\partial N}{\partial T_{fm}}$$

is given by,

$$\frac{\partial N}{\partial T_{fm}} = -\frac{ae}{T_{fm}} \left(b + \frac{c}{d}\right)^{-1} + \frac{ae}{2d \left(b + \frac{c}{d}\right)^2 T_{fm}} + \frac{a}{\left(b + \frac{c}{d}\right)} \frac{dP_{fm}}{dT_{fm}} - \frac{ad^2 ef}{4T_{fm}} + \frac{ad^2 f}{4P_{fm}} (P_{fm} + e) \frac{dP_{fm}}{dT_{fm}} \quad (6)$$

where,

$$a = \frac{\varepsilon}{\tau \delta T_{fm}}, e = (P_{fm} - P_{pm})$$

Since the liquid gets vaporized at the membrane surface, the saturated vapor pressure is given by Clausius-Clapeyron equation including activity coefficient,

$$\frac{dP_{fm}}{dT_{fm}} = \frac{(1-x)\gamma\lambda M P_{fm}^0}{RT_{fm}^2} \quad (7)$$

where

$$P_{fm} = (1-x)\gamma P_{fm}^0$$

and saturation pressure is given by the well known Antoine equation for water:

$$\ln P_{fm}^0 = 23.1964 - \frac{3816.44}{T_{fm} - 46.13} \quad (8)$$

The activity coefficient for saline water is (Lawson and Lloyd 1997),

$$\gamma = 1 - 0.5x - 10x^2 \quad (9)$$

Sensitivity of mass flux to the feed flow rate is given by

$$S(N, Q) = \frac{\partial T_{fm}}{\partial Q} \frac{Q}{T_{fm}} \frac{\partial (\ln N)}{\partial (\ln T_{fm})} = \frac{\partial T_{fm}}{\partial Q} \frac{Q}{T_{fm}} S(N, T_{fm}) \quad (10)$$

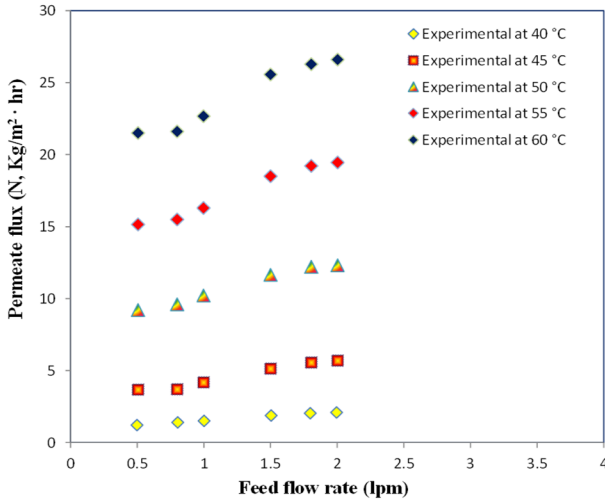


Fig. 2 Effect of feed flow rate on permeate flux [5.5 kPa of permeate pressure and feed salt concentration of 20000 ppm]

Sensitivity of mass flux to the feed bulk temperature is given by

$$S(N, T_f) = \frac{\partial \ln N}{\partial \ln T_f} = \frac{T_f}{N} \frac{\partial N}{\partial T_f} \quad (11)$$

$$\Rightarrow S(N, T_f) = \frac{\partial \ln T_{fm}}{\partial \ln T_f} S(N, T_{fm})$$

Sensitivity of mass flux to the salt concentration is,

$$S(N, x) = \frac{(30x^3 - 19x^2 - 1.5x)P_{fm}^0}{(10x^3 - 9.5x^2 - 1.5x + 1)P_{fm}^0 - P_{pm}} \quad (12)$$

To improve the performance of process, it is important to investigate the process sensitivity to each operating parameter as an input variable. It is necessary to enhance the VMD flux by analyzing the importance of process parameters. The sensitivity of these parameters such as feed flow rate, feed bulk temperature, permeate pressure, feed salt concentration, membrane pore diameter, membrane characteristics with respect to mass flux were determined by using equations (2) to (12).

3.2 Results of sensitivity analysis

3.2.1 Sensitivity of mass flux to feed flow rate

The effect of feed flow rate on trans-membrane flux is shown in Figure 2 at various feed bulk temperatures under permeate pressure of 5.5 kPa. It can be seen that the flux increases linearly at low temperature with increase in feed flow rate but it increases as S-shaped profile at higher temperatures of 55°C and 60°C. Moreover, the permeate flux also increases upon increasing the feed bulk temperature from 40 to 60°C.

Normalized sensitivity factor $S(N, Q)$ on feed flow rate at temperatures varying from 40 to 60°C is shown in Figure 3 at the permeate pressure of 5.5 kPa. It is observed that the system is insensitive at approximately 2 lpm and much sensitive at 1.5 lpm for various feed temperatures.

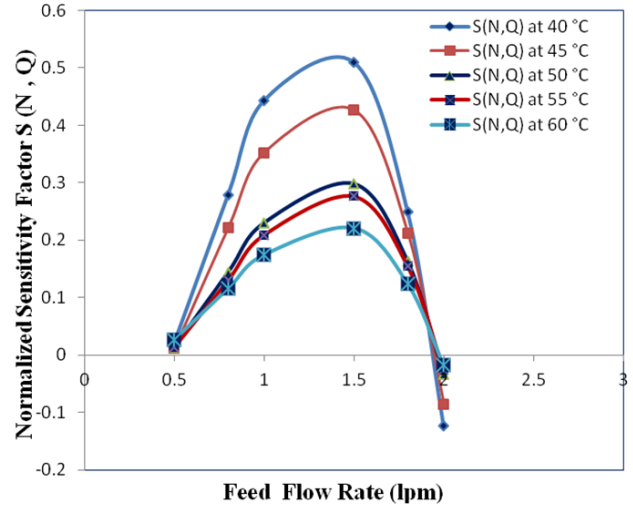


Fig. 3 Effect of feed flow rate on normalized sensitivity $S(N, Q)$ at 5.5 kPa

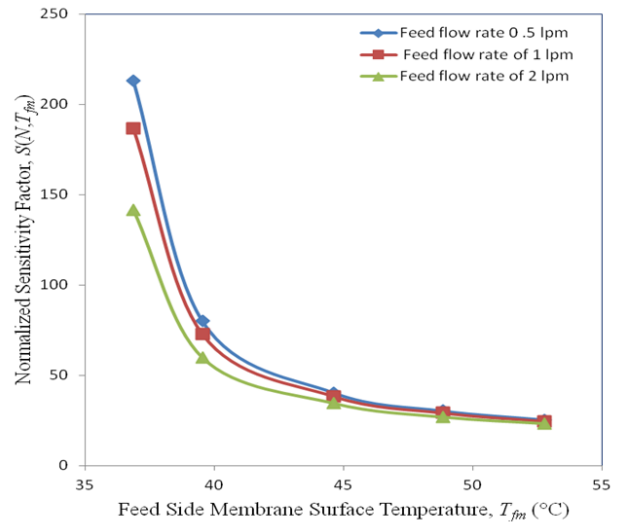
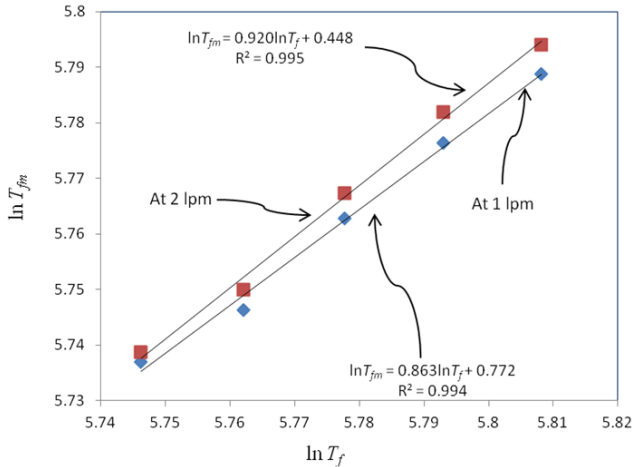
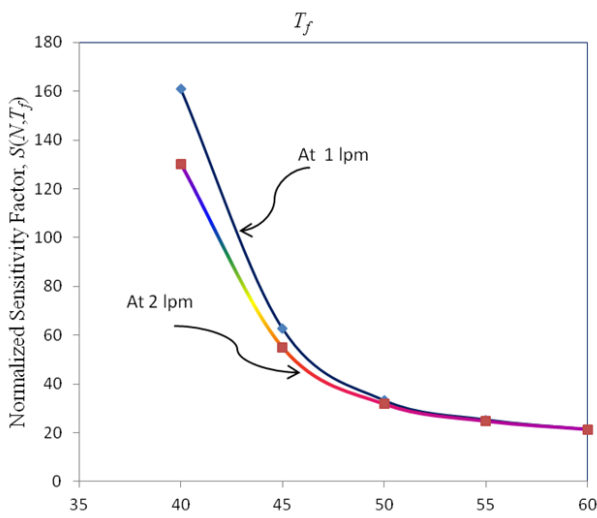


Fig. 4 Effect of feed side membrane temperature on normalized sensitivity $S(N, T_{fm})$

The trend shows that the system sensitivity increases for flow rate from 0.5 lpm to 1.5 lpm and then gradually decreases on increasing flow rate and becomes zero at 2 lpm. The VMD performance is optimum at 2 lpm since the system is nearly insensitive at this feed flow rate. The reason of insensitivity at this flow rate is due to the fact that beyond 2 lpm, the VMD flux is nearly constant, which can be observed experimentally in Figure 2.

3.2.2 Sensitivity of mass flux to feed inlet and feed side membrane temperature

The sensitivity of permeate flux to the feed side membrane and feed bulk temperature is depicted by normalized sensitivity factor. The normalized sensitivity factor of mass flux to feed side membrane temperature and feed bulk temperature were computed using the developed model equations (1), (5) to (9) and (11) simultaneously. The simulated result of Normalized sensitivity $S(N, T_{fm})$ is shown in Figure 4. For computing $S(N, T_f)$, first feed side

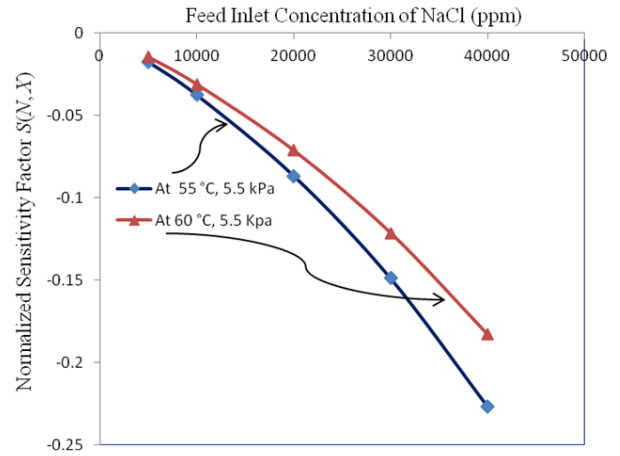
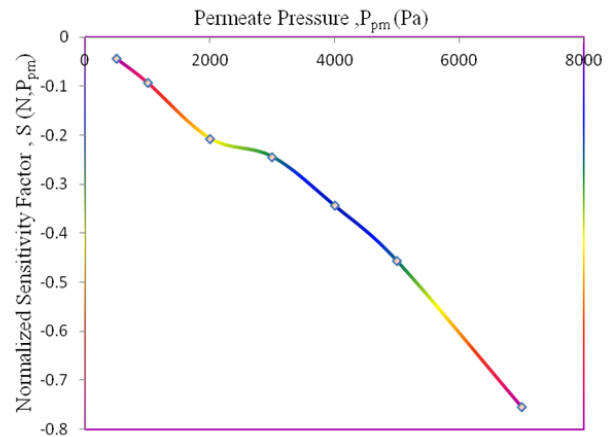
Fig. 5 Fitting of $\ln T_{fm}$ with $\ln T_f$ Fig. 6 Effect of feed bulk temperature (T_f) on normalized sensitivity $S(N, T_f)$ at permeate pressure of 5.5 kPa

membrane temperature, T_{fm} was estimated by using a CFD software Fluent at different feed bulk temperatures, T_f as plotted in Figure 5. A linear relationship between $\ln(T_{fm})$ and $\ln(T_f)$ was fitted as follows:

$$\ln(T_{fm}) = 0.863 \ln(T_f) + 0.772 \text{ at 1 lpm} \quad (13)$$

$$\ln(T_{fm}) = 0.920 \ln(T_f) + 0.448 \text{ at 2 lpm} \quad (14)$$

$S(N, T_f)$ is plotted in Figure 6 at feed flow rate of 1 and 2 lpm at 5.5 kPa of permeate pressure. It is observed from these results that both $S(N, T_f)$ and $S(N, T_{fm})$ remain positive and decrease on increasing the feed bulk temperature. The probable reason may be because of small flux at lower feed temperature, which was also observed experimentally and reported by other researchers (Banat *et al.* 2003). Due to this, any infinitesimally change in feed bulk temperature leads to a large variation in normalized sensitivity. It is observed that system is much sensitive at feed bulk temperature of 40°C and its sensitivity decreases gradually as the temperature of feed increases. It is obvious from the various simulated results as shown in the figure that the VMD set up should be run at higher feed bulk temperature

Fig. 7 Effect of feed concentration on normalized sensitivity $S(N, x)$ at 5.5 kPa of permeate pressureFig. 8 Effect of permeate pressure (P_{pm}) on normalized sensitivity factor $S(N, P_{pm})$

as the system sensitivity is lower and flux is higher, which results in better performance of VMD.

3.2.3 Response of sensitivity on feed salt concentration

The normalized sensitivity factor of mass flux $S(N, x)$ to feed salt concentration was simulated using the developed mathematical model equations (7) to (9) and (12) simultaneously at different feed inlet temperature, feed flow rate of 2 lpm at 5.5 kPa. The trend of sensitivity to feed salt concentration for two different feed inlet temperatures is shown in Figure 7 at 2 lpm of feed flow rate and 5.5 kPa of permeate pressure. It is observed from the results that normalized sensitivity of the mass flux to feed salt concentration remains negative on increasing the salt concentration from 5 g/l to 40 g/l in feed solution. This may be due to the opposite change in mass flux with respect to salt concentration. It is obvious from the simulated results that the sensitivity is lower at lower feed salt concentration. Therefore, the VMD performance is higher at low feed salt concentration and high feed temperature.

3.2.4 Response of sensitivity to permeate pressure

The normalized sensitivity to permeate pressure was

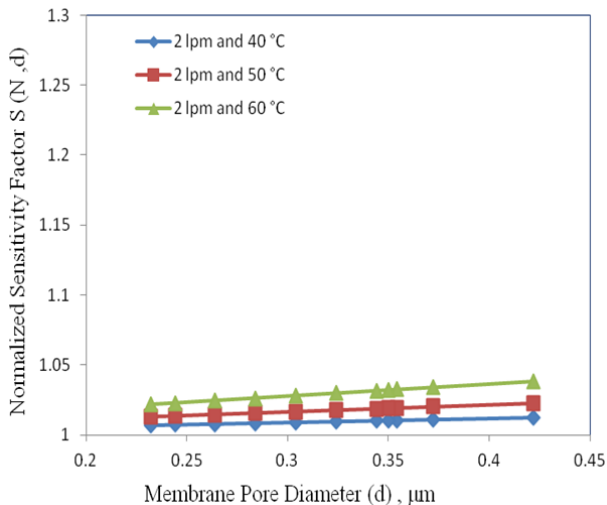


Fig. 9 Effect of membrane pore diameter (d) on normalized sensitivity $S(N, d)$ at permeate pressure of 5.5 kPa

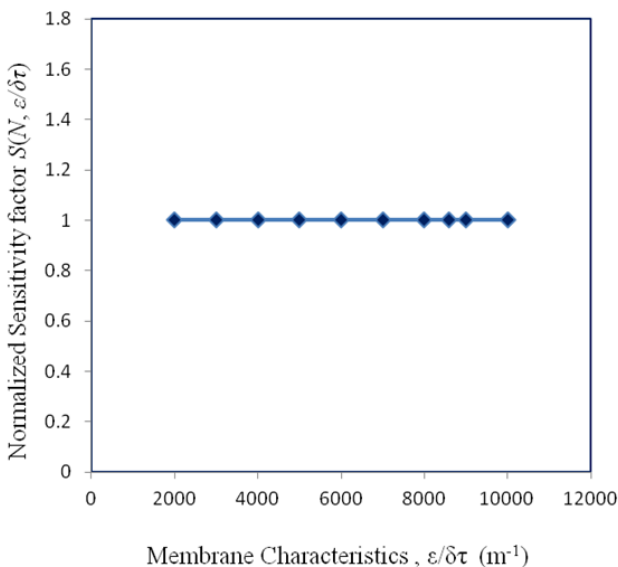


Fig. 10 Response of normalized sensitivity $S(N, \epsilon/\delta\tau)$ to the membrane characteristics ($\epsilon/\delta\tau$) at permeate pressure of 5.5 kPa

computed as shown in Figure 8 at 2 lpm of feed flow rate and 60°C feed bulk temperature. Since the permeate flux decreases on increasing the permeate pressure, the sensitivity is negative. The system is less sensitive at low permeate pressure and the permeate flux is also more; therefore, it should be operated at high vacuum as far as possible.

3.2.5 Response of sensitivity on membrane pore diameter

The normalized sensitivity factor of mass flux $S(N, d)$ to membrane pore diameter was simulated using the developed mathematical model equations (1), (3), (7) to (9) simultaneously at feed inlet temperatures of 40, 50, and 60 °C, 5.5 kPa of permeate pressure and feed flow rate of 2 lpm. The pore diameter was varied from 0.22 μm to 0.43

μm . The simulated results obtained are shown in Figure 9. It can be observed that the normalized sensitivity does not change much and is close to unity indicating almost linear behaviour of mass flux with respect to the pore diameter. This behavior shows that trans-membrane flux is proportional to pore diameter, indicating that Knudsen diffusion is more prevailing as compared to Poiseuille flow, which is also expected as the Knudsen number $K_n = \lambda/d$ is in the range of 0.3-0.63.

3.2.6 Response of normalized sensitivity to membrane characteristics:

The effect of membrane characteristics $\epsilon/\tau\delta$ on trans-membrane sensitivity is shown in Figure 10. There is remarkable variation in mass flux on changing the membrane characteristics $\epsilon/\tau\delta$ from 2000 to 10000. The behaviour shows that trans-membrane flux is proportional to $\epsilon/\tau\delta$. The sensitivity remains constant at 1 (equation 2) because of the linear change in mass flux, which is also evident from equation 1.

4. Taguchi approach

4.1 Analysis of experimental data

Taguchi design philosophy continually strives to reduce variation around the target value. This design methodology involves two steps: the first step towards improving quality is to achieve the population distribution as close to the target value as possible. To achieve this, Taguchi designed experiments using especially constructed tables known as ‘‘Orthogonal arrays (OA)’’ (Oktem et al. 2007). The use of these tables makes the design of experiments vary easy and consistent and a second objective is to develop standard techniques for analysis of results. Through the use of ‘‘outer arrays’’, Taguchi devised an effective way to study the influence of noise factors (uncontrollable sources) such as weather condition, machinery wears, etc. with the least number of repetitions. The end result is the robust design affected minimally by noise factors. Taguchi experimental design usually involves attempting to optimize a process which can involve several factors (e.g., time, temperature, chemical composition etc.) at several levels. Taguchi L_9 involves four process parameters in three levels. The number 9 in the designation OA9 represents the number of rows, which is also the number of treatment conditions. Each row represents a trial condition with factor levels indicated by numbers in the rows. The levels of the factors are permeate pressure (5.5, 6.5, 7 kPa.), feed bulk temperature (45, 55, 60°C), feed flow rate (0.5, 1, 2 lpm) and salt concentration (5, 10, 20 g/l), respectively shown in Table 2 as orthogonal array consisting parameters and its level with the corresponding permeate flux. Each run was conducted twice to study the effects of noise sources on the performance of the VMD setup.

The signal- to- noise (S/N) ratios contribution were chosen as a proactive equivalent to the reactive loss function and to analyze the outcomes. For robust (optimal) design, the S/N ratio represented by Equation (15) should be maximized for system optimization so that response (permeate flux) gets maximized.

Table 2 Taguchi L₉ orthogonal array for experimental data of permeate flux

Run	Feed Bulk Temperature T_f (°C)	Vacuum Degree P_{pm} (kPa)	Feed Flow Rate Q (lpm)	Concentration C (ppm)	Permeate Flux (kg/m ² h)		Mean	SN ratio
					Trial 1	Trial 2		
1	45	7	0.5	5000	2.98	3.24	3.11	9.83
2	45	6.5	1	10000	3.88	4.10	3.99	12.01
3	45	5.5	2	20000	5.44	5.96	5.70	15.09
4	55	7	1	20000	15.15	15.43	15.29	23.69
5	55	6.5	2	5000	18.14	18.40	18.27	25.23
6	55	5.5	0.5	10000	15.10	15.22	15.16	23.62
7	60	7	2	10000	25.52	25.70	25.61	28.17
8	60	6.5	0.5	20000	20.30	20.50	20.40	26.19
9	60	5.5	1	5000	22.57	22.79	22.68	27.11

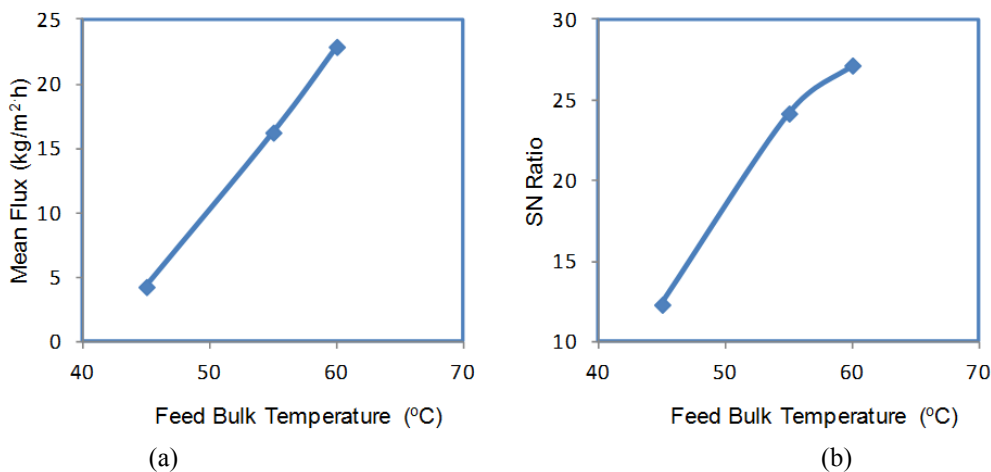


Fig. 11 Effect of feed bulk temperature on (a) permeate flux and (b) SN ratio

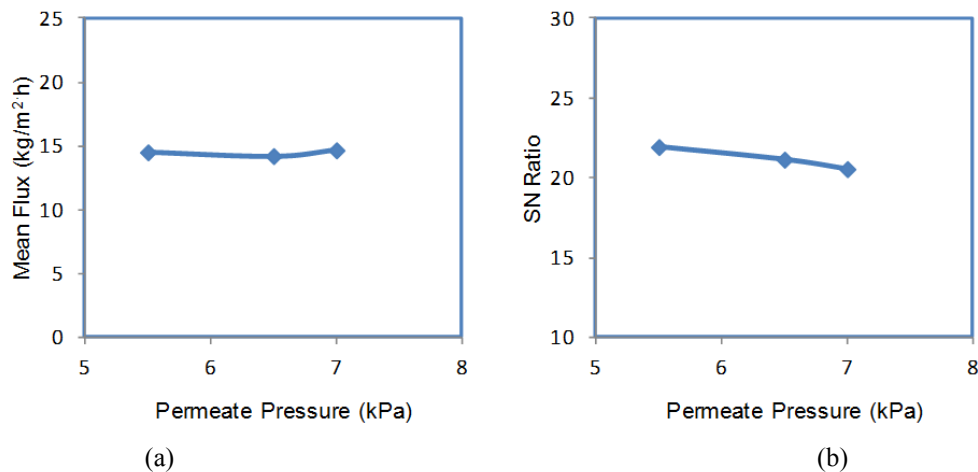


Fig. 12 Effect of permeate pressure on (a) permeate flux and (b) SN ratio

$$S/N = \frac{\text{Amount of energy for intended function}}{\text{Amount of energy wasted}} \quad (15)$$

$$= \frac{\text{signal}}{\text{noise}} = -10 \log \left(\frac{1}{n} \sum_{i=1}^n \frac{1}{y_i^2} \right)$$

where, n is the number of experiments and y_i is the response (permeate flux) of each set of experiment.

In this work, the desalination experiment was performed through VMD set up and the idea was focused for desalination by VMD to increase the trans-membrane permeate flux using robust design process parameter optimization methodology.

4.2 Results of Taguchi approach of experimental data

The effect of feed bulk temperature on outcome (permeate flux) and SN ratio is shown in Figure 11. From

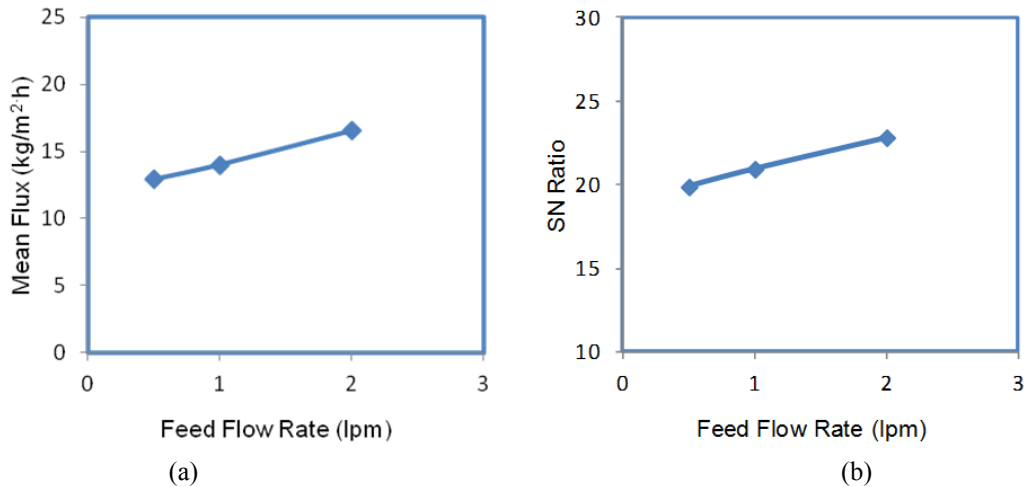


Fig. 13 Effect of feed flow rate on (a) permeate flux and (b) SN ratio

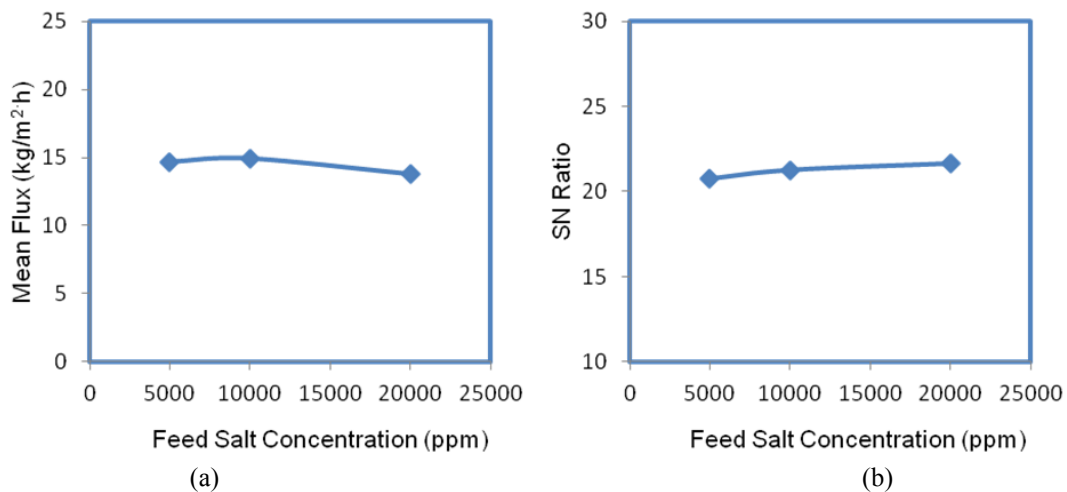


Fig. 14 Effect of salt concentration on (a) permeate flux and (b) SN ratio

this figure, it is obvious that on increasing feed bulk temperature, the mean permeate flux increases from 4.3 to 22.9 kg/m²·h and SN ratio increases from 12.3 to 27.2. Therefore, for maximum permeate flux and SN ratio, the optimum value of feed inlet temperature is 60°C. The effect of permeate pressure on permeate flux and SN ratio is shown in Figure 12. The mean permeate flux does not vary much for the permeate pressure in the range of 5.5 to 7 kPa, however, SN ratio is high at low permeate pressure. Therefore, low permeate pressure is desirable. Figure 13 shows the effect of feed flow rate on permeate flux and SN ratio. On increasing the feed flow rate from 0.5 to 2 lpm, the mean permeate flux increases from 12.9 to 16.5 kg/m²·h and SN ratio increases from 19.9 to 22.8. Therefore, the optimum value of feed flow rate is found to be 2 lpm. The effect of salt concentration on mean permeate flux and SN ratio is shown in Figure 14. There is not much variation in the flux and SN ratio. However, lower concentration favors the permeate flux slightly. At 5.5 kPa of permeate pressure, 60°C of feed inlet temperature, 2 lpm of feed flow rate and 5000 ppm of feed NaCl concentration, the permeate flux was found to be 26.6 kg/m²·h and rejection in the retentate was found to be nearly 99.7%. Electrical conductivity of

permeate was found to be in between 0.05 to 0.1 μS/cm.

4.3 Analysis of variance for experimental data

The aim of analysis of variance (Anova) is to evaluate the significance of process parameters on permeate flux. Percent contribution of variance can be calculated as dependent on the following equations (Oktem *et al.* 2007, Roy Ranjit 1990):

$$\text{Total degree of freedom, } f_T = nr - 1 \quad (16)$$

$$\text{Degree of freedom of input variable, } f_j = \text{Number of levels} - 1 \quad (17)$$

$$\text{Degree of freedom of error, } f_e = f_T - \sum_{j=1}^m f_j \quad (18)$$

$$\text{Correction factor, } CF = \frac{\left(\sum_{i=1}^n y_i \right)^2}{n} \quad (19)$$

$$\text{Total Sum of squares, } SS_T = \sum_{i=1}^n y_i^2 - CF \quad (20)$$

where y_i is the mean of trials, n is the number of experimental runs, r is the number of repetitions, and m is the total number of input variables.

Sum of squares of input variables A (Temperature), B (Permeate Pressure), C (Feed flow rate), D (Feed salt concentration) are:

$$SS_A = A_1^2/N_{A1} + A_2^2/N_{A2} + A_3^2/N_{A3} - CF \quad (21)$$

$$SS_B = B_1^2/N_{B1} + B_2^2/N_{B2} + B_3^2/N_{B3} - CF \quad (22)$$

$$SS_C = C_1^2/N_{C1} + C_2^2/N_{C2} + C_3^2/N_{C3} - CF \quad (23)$$

$$SS_D = D_1^2/N_{D1} + D_2^2/N_{D2} + D_3^2/N_{D3} - CF \quad (24)$$

where A_1, A_2, A_3 are sum of mean values of flux corresponding to temperature of 45, 55, 60°C, respectively. Similarly, $B_1, B_2, B_3, C_1, C_2, C_3, D_1, D_2, D_3$ can be computed.

Mean of squares is given by $MS = SS / \text{DOF}$, where DOF is degree of freedom. F-value is computed by,

$$F = MS / \text{MS of error} \quad (25)$$

$$\text{Percentage contribution, } P = SS / \text{Total SS} \quad (26)$$

The results of ANOVA as calculated from the above equations are shown in Table 3. It can be observed from this table that feed temperature, permeate pressure, feed flow rate, and feed salt concentration influence permeate flux by 95.81%, 0.045%, 3.73%, and 0.354%, respectively.

4.4 Analysis of variance for mathematical model simulated data

In the experimental results, the minimum permeate pressure was limited to 5.5 kPa. To study the contribution of permeate pressure at low values, it was necessary to find the results at low permeate pressures. Therefore simulated results were obtained from the developed mathematical model (Upadhyaya *et al.* 2016a) for the orthogonal array as given in Table 4.

ANOVA results for the simulated data are shown in Table 5. For calculation of F value, the denominator was taken as lowest value of MS since degree of freedom of error is zero. It was found that the percent contribution of permeate pressure on permeate flux gets enhanced up to 5.384% in the range of 2 -7 kPa of permeate pressure. This sudden enhancement in percent contribution is because of increase in vapor pressure difference by increasing the degree of vacuum thereby increase in vaporisation rate. Also, the mass transfer resistance gets reduced by decreasing the permeate pressure on the downstream side since the condensate film thickness gets reduced on decreasing the permeate pressure.

5. Conclusions

An experimental study of VMD process was conducted for analyzing the sensitivity of feed flow rate, permeate

Table 3 Analysis of variance for percent contribution for experimental runs

Factors	DOF	SS	MS	F	P
A	2	534.66	267.33	7138.31	95.810
B	2	0.2519	0.12595	3.363	0.045
C	2	20.8166	10.4083	277.925	3.730
D	2	1.9740	0.987	26.3551	0.354
Error	9	0.3371	0.03745	1	
Total	17	558.0396			

Table 4 Taguchi L_9 orthogonal array for simulated runs using mathematical model

Simulation Run	Feed Bulk Temperature Tf (°C)	Vacuum Degree Ppm (kPa)	Feed Flow Rate Q (lpm)	Concentration C (ppm)	Permeate Flux (kg/m ² h)
1	45	2	0.5	5000	9.61
2	45	5	1.0	10000	5.80
3	45	7	2.0	20000	4.88
4	55	2	1	20000	18.9
5	55	5	2	5000	17.3
6	55	7	0.5	10000	15.0
7	60	2	2	10000	25.0
8	60	5	0.5	20000	23.0
9	60	7	1.0	5000	21.8

Table 5 Analysis of variance for percent contribution for simulated runs using mathematical model

Factors	DOF	SS	MS	F	P
A	2	416.9587	208.47935	1996.92864	94.238
B	2	23.8215	11.91075	114.0876	5.384
C	2	0.2088	0.1044	1	0.047
D	2	1.4615	0.73075	6.999	0.330
Error	0	0	-	-	-
Total	8	442.4505			

pressure, feed bulk temperature and feed salt concentration on trans-membrane permeate flux. VMD performance was found to be optimum at feed flow rate of 2 lpm, feed bulk temperature of 60°C, low permeate-side pressure and lowest salt concentration. Normalized sensitivity remains positive at 1 in the range of 2000 to 10000 m⁻¹ of membrane characteristics parameter, which indicates that permeate flux will increase on increasing the membrane characteristics parameter.

The process parameters were also studied using Taguchi optimization method for both experimental and simulated data. It was found that the optimum values of process parameters are similar in the lines of those obtained by sensitivity analysis. Under the optimum conditions, the experimental permeate flux was found to be 26.6 kg/m²·h and rejection in the retentate was found to be nearly 99.7%. Further, ANOVA analysis was carried out for determining the percent contribution of process parameters. It was found that the most important parameter is feed temperature with

percent contribution as 95% approximately on permeate flux. The percent contribution of permeate pressure was found to be 0.045% in the range of 5.5 to 7 kPa, however, this contribution showed remarkable increment (5.384%) on reducing the permeate pressure to 2 kPa.

References

- Abu-Zeid, M.A.E.R., Zhang, Y., Dong, H., Zhang, L., Chen, H.L. and Hou, L. (2015), "A comprehensive review of vacuum membrane distillation technique", *Desalination*, **356**, 1-14.
- Alkudhiri, A., Darwish, N. and Hilal, N. (2012), "Membrane distillation: A comprehensive review", *Desalination*, **287**, 2-18.
- Banat, F., Al-Rub, F.A. and Bani-Melhem, K. (2003), "Desalination by vacuum membrane distillation: Sensitivity analysis", *Separat. Purif. Technol.*, **33**(1), 75-87.
- Bandini, S., Saavedra, A. and Sarti, G.C. (1997), "Vacuum membrane distillation: Experiments and modeling", *AIChE J.*, **43**(2), 398-408.
- Bandini, S. and Sarti, G.C. (1999), "Heat and mass transport resistances in vacuum membrane distillation per drop", *AIChE J.*, **45**(7), 1422-1433.
- Bouguecha, S., Chouikh, R. and Dhahbi, M. (2003), "Numerical study of the coupled heat and mass transfer in membrane distillation* 1", *Desalination*, **152**(1-3), 245-252.
- Chaurasia, S.P., Upadhyaya, S. and Singh, K. (2013), "Water desalination by vacuum membrane distillation", *AIChE Annual Meeting*, San Francisco, U.S.A., November.
- Criscuoli, A., Bafaro, P. and Drioli, E. (2013), "Vacuum membrane distillation for purifying waters containing arsenic", *Desalination*, **323**, 17-21.
- El-Bourawi, M.S., Ding, Z., Ma, R. and Khayet, M. (2006), "A framework for better understanding membrane distillation separation process", *J. Membr. Sci.*, **285**(1-2), 4-29.
- Izquierdo-Gil, M.A., Fernandez-Pineda, C. and Lorenz, M.G. (2008), "Flow rate influence on direct contact membrane distillation experiments: Different empirical correlations for Nusselt number", *J. Membr. Sci.*, **321**(2), 356-363.
- Izquierdo-Gil, M.A. and Jonsson, G. (2003), "Factors affecting flux and ethanol separation performance in vacuum membrane distillation (VMD)", *J. Membr. Sci.*, **214**(1), 113-130.
- Khayet, M. (2011), "Membranes and theoretical modeling of membrane distillation: A review", *Adv. Colloid Interface Sci.*, **164**(1), 56-88.
- Kuram, E., Tasci, E., Altan, A.I., Medar, M.M., Yilmaz, F. and Ozcelik, B. (2013), "Investigating the effects of recycling number and injection parameters on the mechanical properties of glass-fibre reinforced nylon 6 using Taguchi method", *Mater. Design*, **49**, 139-150.
- Lawson, K.W. and Lloyd, D.R. (1997), "Membrane distillation", *J. Membr. Sci.*, **124**(1), 1-25.
- Lovineh, S.G., Asghari, M. and Rajaei, B. (2013), "Numerical simulation and theoretical study on simultaneous effects of operating parameters in vacuum membrane distillation", *Desalination*, **314**, 59-66.
- Mehat, N.M. and Kamaruddin, S. (2011), "Investigating the effects of injection molding parameters on the mechanical properties of recycled plastic parts using the Taguchi method", *Mater. Manufact. Processes*, **26**(2), 202-209.
- Mengual, J.I., Khayet, M. and Godino, M.P. (2004), "Heat and mass transfer in vacuum membrane distillation", *J. Heat Mass Transfer*, **47**(4), 865-875.
- Mohammadi, T. and Safavi, M.A. (2009), "Application of Taguchi method in optimization of desalination by vacuum membrane distillation", *Desalination*, **249**(1), 83-89.
- Naidu, G., Choi, Y., Jeong, S., Hwang, T.M. and Vigneswaran, S. (2014), "Experiments and modeling of a vacuum membrane distillation for high saline water", *J. Industrial Eng. Chem.*, **20**(4), 2174-2183.
- Oktem, H., Erzurumlu, T. and Uzman, I. (2007), "Application of Taguchi optimization technique in determining plastic injection molding process parameters for a thin-shell part", *Mater. Design*, **28**(4), 1271-1278.
- Pangarkar, B.L., Parjane, S.B., Abhang, R.M. and Guddad, M. (2010), "The heat and mass transfer phenomena in vacuum membrane distillation for desalination", *J. Chem. Biomolecular Eng.*, **3**(1), 33-38.
- Roy Ranjit, K. (1990), *A Primer on Taguchi Method*, Van Nostrand Reinhold, New York, U.S.A.
- Shim, S.M., Lee, J.G. and Kim, W.S. (2014), "Performance simulation of a multi-VMD desalination process including the recycle flow", *Desalination*, **338**, 39-48.
- Soni, V., Abildskov, J., Jonsson, G. and Gani, R. (2008), "Modeling and analysis of vacuum membrane distillation for the recovery of volatile aroma compounds from black currant juice", *J. Membr. Sci.*, **320**(1), 442-455.
- Upadhyaya, S., Singh, K., Chaurasia, S.P., Dohare, R.K. and Agarwal, M. (2016a), "Mathematical and CFD modeling of vacuum membrane distillation for desalination", *Desalination Water Treat.*, **57**(26), 11956-11971.
- Upadhyaya, S., Singh, K., Chaurasia, S.P., Dohare, R.K. and Agarwal, M. (2016b), "Recovery and development of correlations for heat and mass transfer in vacuum membrane distillation for desalination", *Desalination Water Treat.*, **57**(55), 26886-26898.
- Varma, A., Morbidelli, M. and Wu, H. (2005), *Parametric Sensitivity in Chemical Systems*, Cambridge University Press, United Kingdom.
- Walton, J., Lu, H., Turner, C., Solis, S. and Hein, H. (2004), "Solar and waste heat desalination by membrane distillation", *Desalination and Water Purification Research and Development Program Report No. 81*, Agreement No. 98-FC-81-0048, U.S. Department of the Interior, Environmental Services Division, Denver, U.S.A.
- Xu, Z., Pan, Y. and Yu, Y. (2009), "CFD simulation on membrane distillation of NaCl solution", *Frontiers of Chemical Engineering in China*, **3**(3), 293-297.

CC

Nomenclature

d	Membrane Pore Diameter(m)
D_{AB}	Diffusivity of A in B (m^2/s), where A is water vapour, and B is air
K_n	Knudsen Number
M	Molecular Weight of Water (kg/kmol)
N	Total Trans – Membrane Flux ($kmol/m^2 \cdot h$)
$N_{A,M-K-P}$	Total Trans – Membrane Flux ($kmol/m^2 \cdot s$)
P_{pm}	Permeate Side Membrane Pressure (kPa)
P_{fm}	Feed Side Membrane Pressure (kPa)
P_{fm}^0	Vapor pressure at feed side membrane (kPa)
R	Universal Gas Constant ($J/kmol \cdot K$)
r	Membrane Pore Radius (m)
T_f	Feed Bulk Temperature (K)
T_{fm}	Feed Side Membrane Surface Temperature (K)

T_{pm}	Permeate Side Membrane Surface Temperature (K)
x	Mole fraction of NaCl in water
y_A	Mole Fraction of Water Vapour

Greek Letters

δ	Membrane Thickness (m)
ε	Membrane Porosity
λ	Latent heat of vaporization of water (J/kmol)
η	Viscosity of Water Vapour (kg/m·s)
τ	Membrane Tortuosity